*Paper No. 260. (quote when citing this article)*
Eleventh World Conference on Earthquake Engineering
ISBN: 0 08 042822 3

# DISTRIBUTION OF ENERGY INPUT AND DISSIPATION ALONG STORIES IN STEEL BUILDING STRUCTURES WITH HYSTERETIC DAMPERS

M. NAKASHIMA and T. MITANI

Disaster Prevention Research Institute, Kyoto University
Gokasho, Uji, Kyoto 611 JAPAN
Department of Construction Engineering, Kobe University
Rokkodai, Nada-ku, Kobe, Hyogo 657 JAPAN

## ABSTRACT

This paper presents an analytical study on the energy input and dissipation behavior of structures with hysteretic dampers made of a low-yield steel. Such structures are characterized by relatively large stiffness after initial yielding and significant isotropic-type hardening. It was found that basic premises of the energy-based design are applicable for such structures and isotropic-type hardening has an effect of making the distribution of dissipated energy along the stories uniform.

## KEYWORDS

hysteretic damper; low-yield steel; energy-based design; isotropic hardening; energy dissipation.

## INTRODUCTION

This study is presented against the background of (1) the growing use of hysteretic dampers for controlling building responses under earthquakes, and (2) the increasing interest in energy-based seismic design. The paper focuses on hysteretic dampers consisting of steel panels (walls) and subjected to in-plane shear under earthquake loading. A sketch of such a damper is illustrated in Fig.1(a) (Nakashima *et al.*, 1994), together with a prototype structure, and the conceptual mechanism on earthquake resistance of such a structure is shown in Fig.2(a). In this figure, the first yielding of the structure corresponds to the yielding of the damper, whereas the second yielding is activated by the yielding of the main frame. It is notable that the stiffness in the second branch relative to the initial elastic stiffness [referred to as the ratio of second stiffness ($\alpha$) hereafter] is a function of the stiffnesses of the main frame (Kf) and the damper (Kd) and given as $\alpha = Kf/(Kf+Kd)$, with the assumption that the damper behaves in a linear-elastic and perfectly-plastic manner. It should be emphasized that, according to previous design applications, the ratio cannot be assigned a small value, i.e., the main frame cannot be designed so flexibly because, given the lateral stiffness provided to the frame in the course of design for vertical loads and others, and the ratio can easily reach more than 0.5.

The idea of energy-based seismic design was first advocated by Housner (1956), and has been examined successively by many researchers [for example, Akiyama (1985)]. Structures with hysteretic dampers rely for their seismic safety on the energy dissipation provided by the dampers, and thus their energy dissipation capacity and demand are of critical concern in seismic design. Considering its capacity to deal explicitly with both the energy dissipation capacity and the energy dissipation demand, the energy-based seismic design method is a very logical choice for the design of structures with hysteretic dampers. In this paper, extensive numerical analysis is carried out to examine whether the basic premises developed for energy-based seismic design are applicable for structures with hysteretic dampers, which are characterized by large second stiffness after yielding, and to investigate how the energy dissipation is distributed among individual hysteretic dampers arranged along the stories.

Another topic of this paper is the use of a low-yield steel for hysteretic (panel) dampers. The low-yield steel under consideration has a yield stress of about 80 MPa, approximately one third that of mild steels, and its use is intended to activate energy dissipation under lower levels of earthquakes. Earlier studies (Nakashima *et al.*, 1994) have shown that hysteretic dampers made of the low-yield steel ensure stable and ductile hysteretic behavior but involve conspicuous isotropic-type hardening [Fig.1(b)]. How such hardening affects the energy input and dissipation characteristics, as well as the distribution of those energies along the stories, is also scrutinized in this paper.

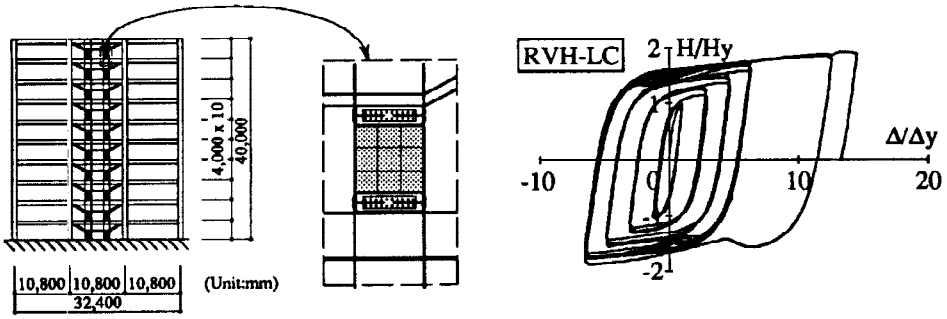


(a) (b)

Fig.1. A sketch of a prototype building with hysteretic (panel) dampers: (a) prototype building; (b) hysteretic curves of prototype hysteretic damper (from Nakashima, *et al.* (1994)).

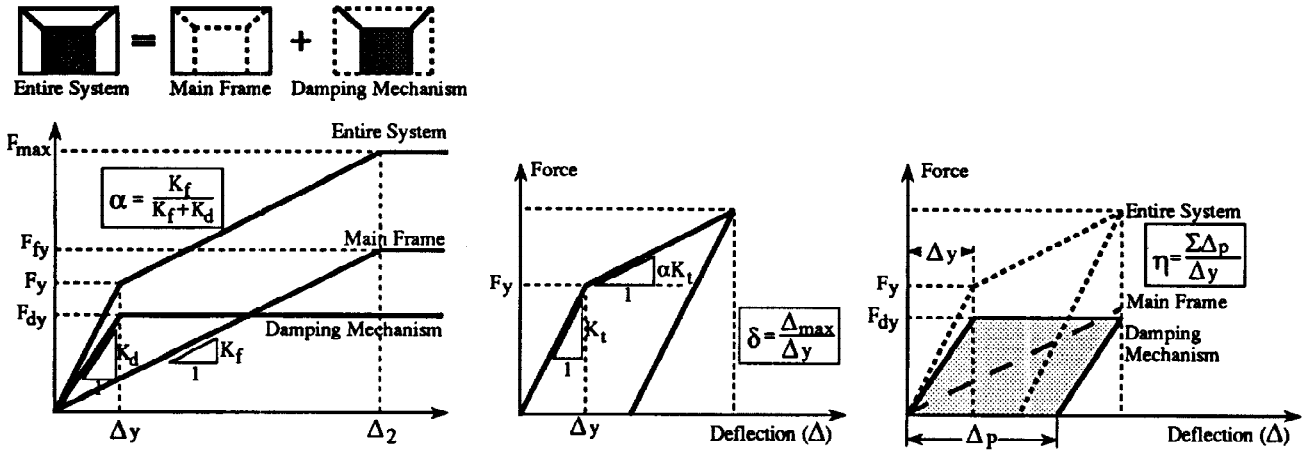


(a) (b) (c)

Fig.2. Conceptual earthquake-resisting mechanism of a structure with hysteretic dampers: (a) basic mechanism; (b) bilinear representation; (c) definition of symbols.

## ENERGY BEHAVIOR OF SYSTEMS HAVING LARGE SECOND STIFFNESS

### Energy Input and Dissipation Behavior of SDOF Systems

To begin with, the energy input and dissipation behavior of SDOF systems that have relatively large second stiffness is examined. The systems analyzed are represented by a bilinear model shown in Fig.2(b) (meaning that the main frame is assumed to behave only linearly). Although the real behavior is rather trilinear [Fig.2(a)], the analysis stuck to the bilinear model because this treatment allows us to examine directly the maximum deflection under which the main frame does not go beyond yielding. [Note that a key goal in the design of structures with hysteretic dampers is to retard the damage (i.e., yielding) to the main frame as much as possible, so that information on the maximum deflection for bilinear systems is crucial.]

The fundamental premise of energy-based seismic design is that the total input and dissipated energies exerted on the structure remain relatively constant regardless of the yield force (Akiyama, 1985). Previous studies have also indicated that these energy terms are relatively independent of the ratio of second stiffness ($\alpha$), but this observation was developed only for systems whose ratios are 0.1 to at most 0.25 (Nakashima *et*

*al.*, 1996). As stated earlier, the ratio tends to be much larger and easily exceeds 0.5 in structures with hysteretic dampers. Numerical step-by-step time integration analysis was carried out to investigate whether those basic premises are still applicable for such structures. Major variables adopted were: (1) the type of ground motions [1940 El-Centro record, 1951 Taft record, 1978 Miyagiken-oki record, and 1995 (Hyogoken-Nanbu Earthquake) Japan Meteorological Agency (JMA) record]; (2) the viscous damping ratio (h = 0.02 to 0.10); (3) the natural period (T = 0.1 to 5.0 sec.); (4) the yield force (Fy) (0.1 to 0.6 in terms of Fy/Fe, with Fe defined as the maximum force exerted if the system would behave only linearly); and (5) the ratio of the second stiffness ($\alpha$ = 0.0 to 0.75). Figures 3 and 4 show representative results obtained from this analysis, indicating that the input and dissipated energies (presented in terms of the equivalent velocities Vt and Vp, respectively) are relatively constant regardless of the values of the yield force and ratio of second stiffness and that the basic premises of energy-based seismic design hold their values for systems with large second stiffness. Details of the analysis and its results are presented elsewhere (Nakashima *et al.*, 1996)

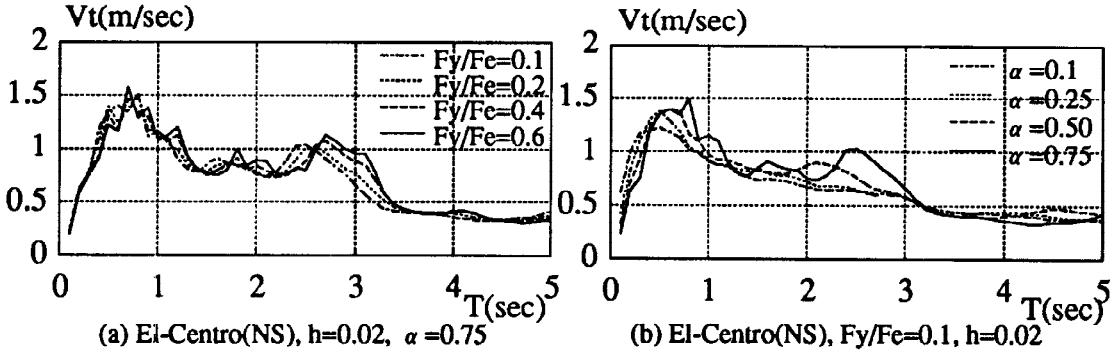


(a) El-Centro(NS), h=0.02, $\alpha$ =0.75 (b) El-Centro(NS), Fy/Fe=0.1, h=0.02

Fig.3. Input energy spectra for various yield strengths and ratios of second stiffnesses.

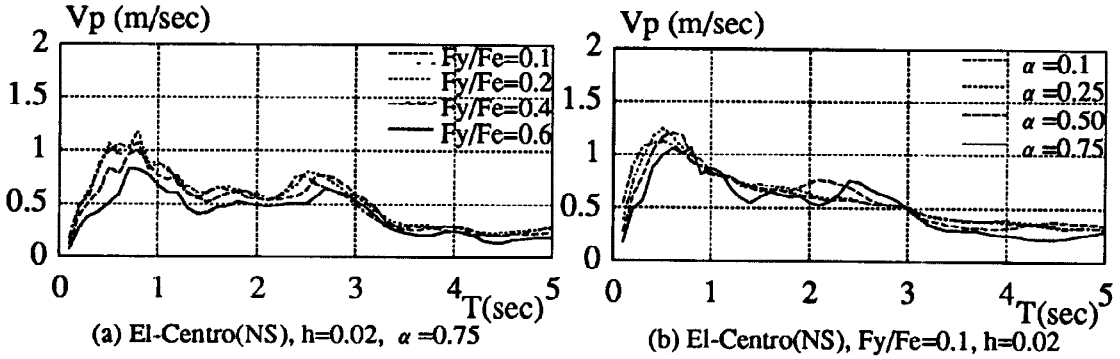


(a) El-Centro(NS), h=0.02, $\alpha$ =0.75 (b) El-Centro(NS), Fy/Fe=0.1, h=0.02

Fig.3. Dissipated energy spectra for various yield strengths and ratios of second stiffnesses.

The dissipated energy ($E_p = 1/2MV_p^2$, with M as the mass of the system) and the ratio of cumulative plastic deformation [$\eta$, defined in Fig.2(c)] can be correlated as:

$$\eta = \frac{E_p}{(1-\alpha)F_y\Delta_y} \tag{1}$$

where (1-$\alpha$)Fy equals the damper's yield force, Fdy [Fig.2(c)]. In the design, if design dissipated energy (Vp) spectra are assigned and a yield force is selected, the required ratio of cumulative plastic deformation can be estimated by Equation (1), and the structure is judged to be safe if the damper is able to absorb this much cumulative plastic deformation without strength deterioration. As noted earlier, the maximum deflection [$\delta$, defined in Fig.2(b)] is also an important index in design, but cannot be estimated explicitly from the above energy consideration. After extensive calibration of the results obtained in this study, the following empirical expression is provided for correlating the ratio of cumulative plastic deflection ($\eta$) with the ratio of maximum deflection ($\delta$):

$$\delta = \sqrt{\eta + 1} \tag{2}$$

Figure 5 shows the correlation between the numerically obtained ratios of maximum deflections (δ) and the ratios of maximum deflection estimated from Equation (2) (δ'), demonstrating that the empirical equation provides a reasonable estimate. As may readily be conceived, the relation between the two quantities (η and δ) is a great deal dependent on the type of ground motions: if ground motions of an impulsive type are applied, the maximum deflection relative to the cumulative plastic deformation becomes larger, whereas this ratio decreases for ground motions of a sinusoidal type and having a long duration. Among the ground motion records used in this study, the JMA Kobe record is of a relatively impulsive type, while other records fall into the category of far-field motions of long duration. Despite the differing types of ground motions employed in the study, Equation (2) gives us a reasonable estimate. More study is needed, however, to verify the effectiveness of this equation.

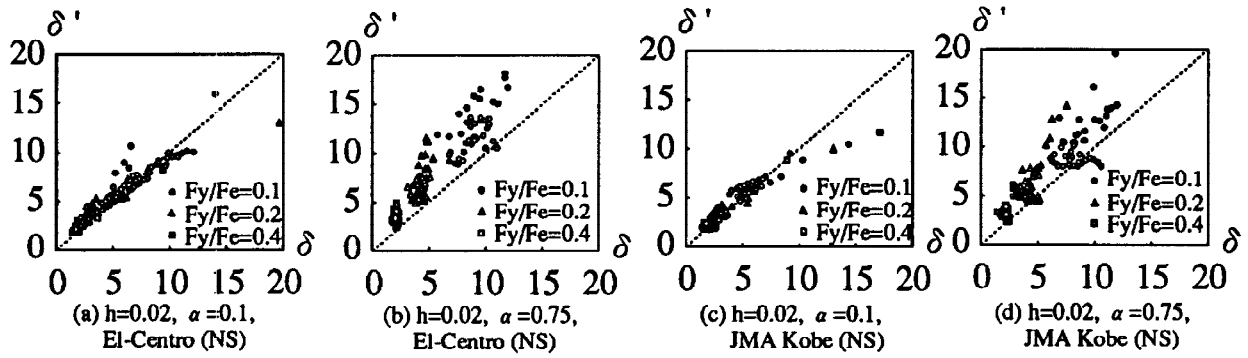


Fig.5. Correlation between numerically obtained maximum deformations (δ) and estimated maximum deformations (δ').

Energy Input and Dissipation Behavior of MDOF Systems

The most fundamental premise of energy-based seismic design for general MDOF systems is that the total input and dissipated energies of an MDOF system are equal to the total input and dissipated energies of an equivalent SDOF system whose mass and natural period equal the total mass and fundamental natural period of the MDOF system. To examine the applicability of this premise to MDOF systems having large second stiffness, a numerical step-by-step time integration was carried out. Assumptions made and variables used in this analysis were the same as those employed for the analysis of SDOF systems. In addition, the story yield force was adjusted so that all stories would yield simultaneously under the design earthquake force profile stipulated in Japan's Seismic Design Specification; the base shear coefficient was set at 0.1 (a smaller value than that normally used was adopted in consideration of possible earlier yielding of hysteretic dampers with the low-yield steel); the story's drift angle was set at 1/800 at yielding; the ratio of second stiffness was constant throughout the stories; and the number of stories was selected as one of 3, 6, 9, 12, 15, 18, or 21.

Figure 6 shows representative results, demonstrating that both the total input and the dissipated energies are close to each other between MDOF and equivalent SDOF systems, even if the ratio of second stiffness is large (up to $\alpha = 0.75$). Figure 7(a) shows distributions of cumulative plastic deformations along the stories for various ratios of second stiffness. Here, $\eta_j$ is the ratio of cumulative plastic deformation for the j-th story, whereas h' is the ratio calculated if all stories are assumed to sustain the same ratio of cumulative plastic deformation. Although the distribution of yield forces along the stories was selected such that they would yield simultaneously under the design earthquake force profile, distributions of cumulative plastic deformations fluctuate rather significantly when the ratio of second stiffness is small [say, $\alpha = 0.1$ in Fig.7(a)], while they are relatively constant for larger ratios. In real design, it is not an easy task to distribute the story yield forces precisely in accordance with the design earthquake force profile because of construction preferences (e.g., a preference for uniform column dimensions for multiple stories). To examine how the distribution of cumulative plastic deformations is affected by the inevitable disturbance of the story yield force distribution, analysis was conducted in which the yield force of one particular story (the 1st, 4th, or 7th story in the 9-story model) was intentionally reduced to 80% of the original. Figures 7(b)-(d) show the results obtained, which demonstrate that the cumulative plastic deformation increases for the weakened story, particularly when the ratio of second stiffness is small. On the other hand, if this ratio exceeds 0.5, the increase is kept small. This condition seems very advantageous from the design viewpoint, because the cumulative plastic deformations demanded of individual hysteretic dampers would not change significantly because of the inevitable fluctuations of the story yield forces. A conclusion to be drawn from

this observation is that keeping the ratio of second stiffness from being too small (by providing relatively large lateral stiffness to the main frame) has the merit of ensuring a more uniform distribution in the cumulative plastic deformation.

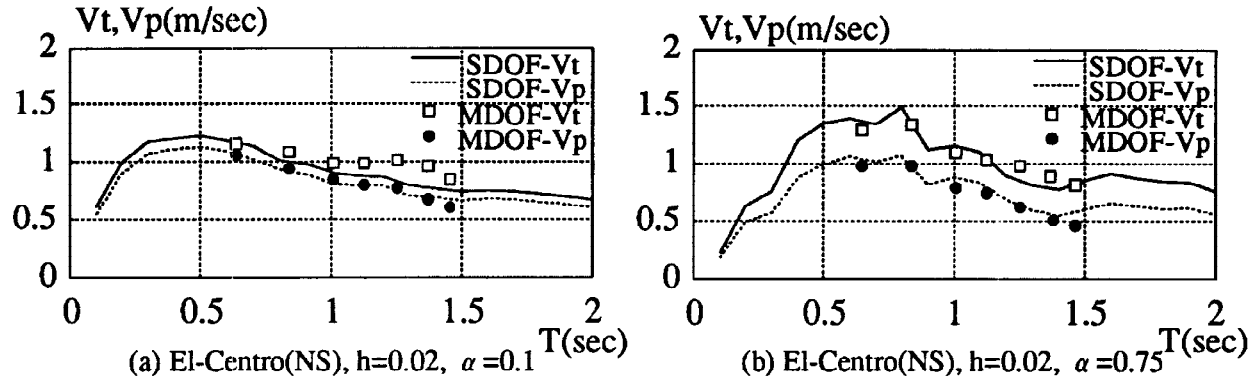


Fig.6. Total input and dissipated energies of MDOF systems and their correlation with equivalent SDOF systems

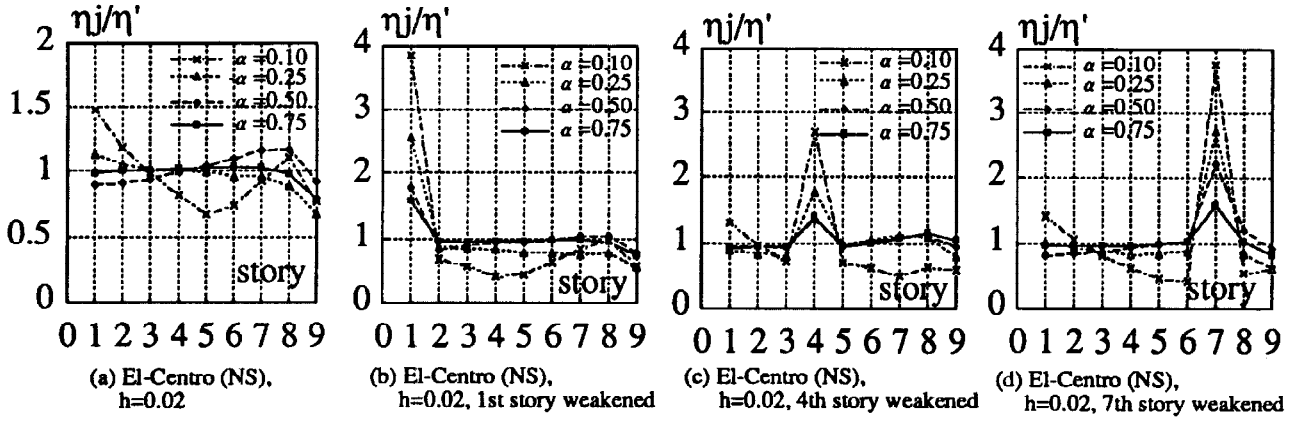


Fig.7. Distribution of cumulative plastic deformations (η) for various ratios of second stiffness.

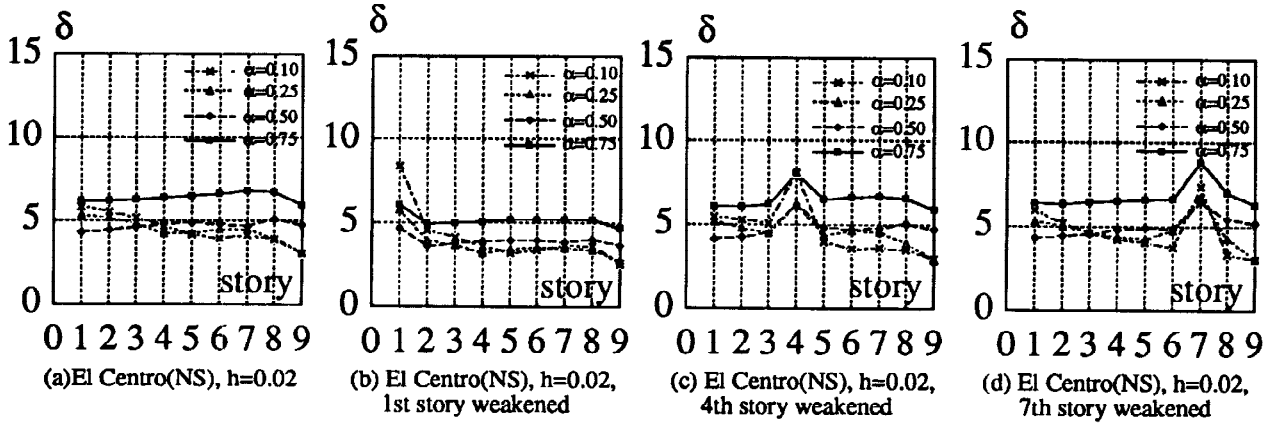


Fig.8. Distribution of maximum deformations (δ) for various ratios of second stiffness.

What about the distribution of maximum deflection (δ)? Figure 8(a) shows distributions of maximum deflections for the 9-story model. Contrary to the corresponding distributions of cumulative plastic deformations [Fig.7(a)], the distributions of maximum deflections remain relatively constant even when the ratio of second stiffness is small. In addition, it is notable that the maximum deflection decreases with the decrease in the ratio of second stiffness. This behavior is understandable because a smaller ratio of second stiffness having the same yield force means that larger hysteretic dampers are installed in the structure and provide larger energy dissipation for the same deflection. When the yield force of one particular story is

weakened, the maximum deflection in that story increases, and this increase is more significant for smaller ratios of second stiffness [Fig.8(b)-(d)]. The degree of increase, however, is not so conspicuous as that observed for the cumulative plastic deformation [Fig.7(b)-(d) against Fig.8(b)-(d)]. In summary, the effect of the ratio of second stiffness on the story distribution is less significant for the maximum deflection than for the cumulative plastic deformation.

## HYSTERETIC BEHAVIOR OF HYSTERETIC DAMPERS MADE OF LOW-YIELD STEEL

Until the previous sections, it was assumed that hysteretic dampers arranged in the frame behave in a linear-elastic perfectly-plastic manner [Fig.2(a)]. The first writer and his associates conducted a series of tests to quantify the hysteretic behavior of shear panels (hysteretic dampers) made of the low-yield steel introduced at the beginning of the paper. A set of hysteretic curves obtained for a full-size shear panel are shown in Fig.1(b), and another set of hysteretic curves obtained for a scaled shear panel in Fig.9(a) (Nakashima *et al.*, 1995). Both results reveal significant isotropic-type hardening under cycles with a specified deflection amplitude as well as under increasing amplitudes. Figure 9(b) shows the accumulation of dissipated energy obtained from the hysteretic curves [Fig.9(a)], together with the progress of dissipated energy if the system behaved in a linear-elastic perfectly-plastic manner. This figure clearly indicates that the bilinear representation significantly underestimates the energy dissipation capacity of hysteretic dampers made of the low-yield steel.

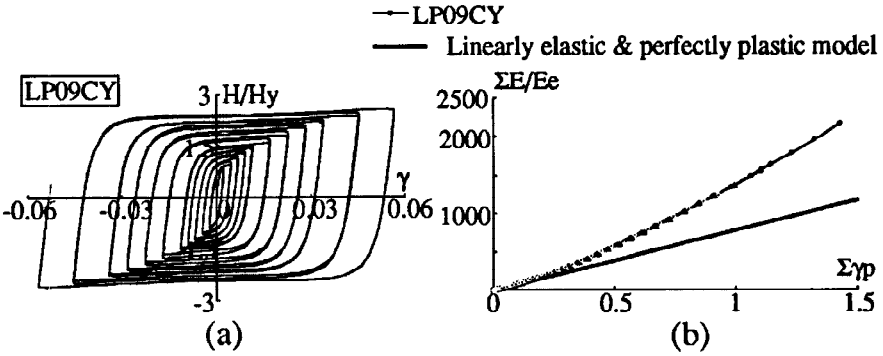


Fig.9. Hysteretic and energy dissipation behavior of hysteretic (panel) dampers (from Nakashima *et al.*, 1995).

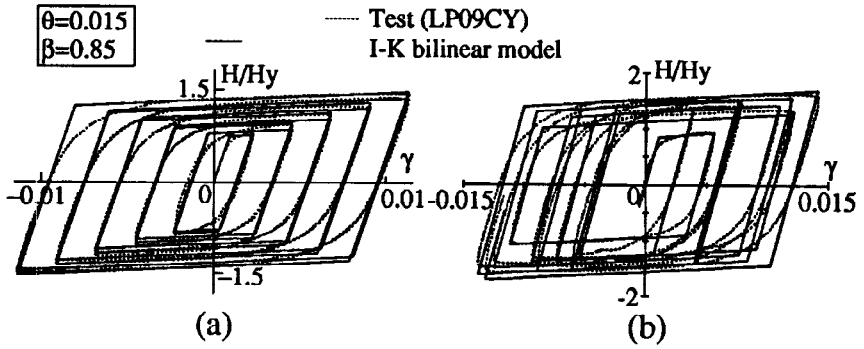


Fig.10. Comparison between experimental and analytical hysteretic behavior: (a) quasi-static test; (b) pseudo dynamic test (from Nakashima *et al.*, 1995(b)).

The first writer developed a simple analysis model that can simulate the significant isotropic-type hardening associated with such dampers [Nakashima *et al.*, 1995(b)]. This model, designated as the I-K bilinear model, is essentially the same as the bilinear model except for an additional parameter that allows for isotropic-type hardening under cycles with a constant amplitude as well as under increasing amplitudes. Comparison between experimental hysteresis curves and hysteresis curves obtained from this model is presented in Fig.10, which includes hysteresis curves created for a predetermined displacement history [Fig.10(a)] and hysteresis curves obtained from a pseudo-dynamic test [Fig.10(b), Nakashima *et al.*, 1995(a)]. Correlation between the experimental and analytical curves has been found to be satisfactory.

## ENERGY BEHAVIOR OF SYSTEMS WITH DAMPERS INVOLVING SIGNIFICANT ISOTROPIC-TYPE HARDENING

### Energy Input and Dissipation Behavior of SDOF Systems

The analysis conducted for bilinear SDOF systems was repeated for SDOF systems into which isotropic-type hardening was incorporated. The main frame was assumed to behave linearly, and the damper's hysteretic behavior was represented by the I-K bilinear model. Comparison between the dissipated energy of the system [expressed in terms of the equivalent velocity (Vpi)] and the dissipated energy of the same system but with the bilinear assumption (Vpk) indicated that, when the ratio of second stiffness is small, Vpi is slightly larger than Vpk, whereas both energies remain essentially the same for large ratios of second stiffness. The latter is understandable because a larger ratio of second stiffness means a smaller damper (a smaller contribution of the damper to the overall response), as discussed earlier. From a practical viewpoint, the energy dissipation characteristics are judged not to change if isotropic-type hardening is present.

In Fig.11, cumulative plastic deformations obtained for systems involving isotropic-type hardening ($\eta i$) are compared to those of the equivalent bilinear systems ($\eta k$). For smaller yield strengths (if compared for the same ratio of second stiffness) as well as for larger ratios of second stiffness (if compared for the same yield strength), the reduction of cumulative plastic deformations is more significant. This observation can be interpreted as follows: the larger the ratio of cumulative plastic deformation is, the more significant is the isotropic-type hardening, which results in a more pronounced increase in the apparent yield strength under repeated loading. On the other hand, such an increase in strength reduces the required ratio of cumulative plastic deformation if the total dissipated energy is assumed to be constant. With this behavior in mind, a smaller yield strength requires a larger ratio of cumulative plastic deformation, and a larger ratio of second stiffness is also accompanied by a smaller yield strength of the dampers. In summary, isotropic-type hardening has a visible effect on the reduction of the cumulative plastic deformation required of hysteretic dampers.

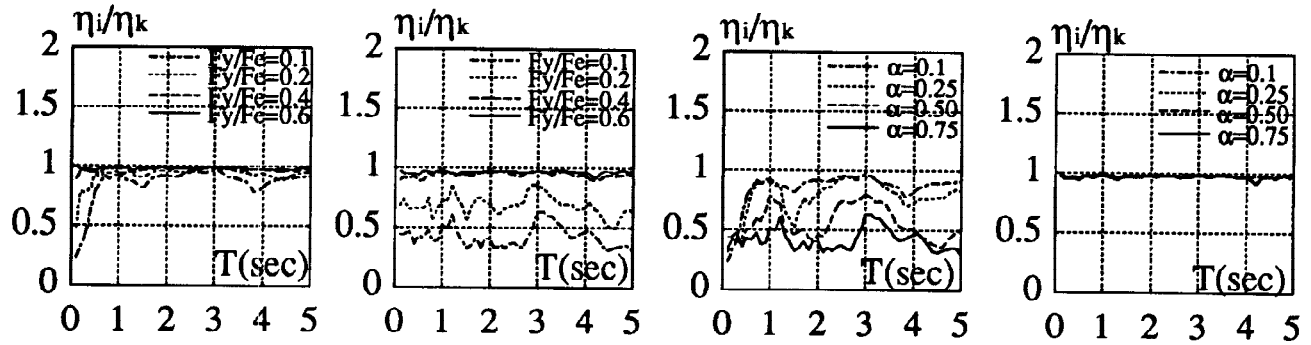


Fig.11. Comparison in cumulative plastic deformation between bilinear ($\eta k$) and I-K bilinear ($\eta i$) models.

### Energy Input and Dissipation Behavior of MDOF Systems

Analysis was repeated for the MDOF systems described earlier, but this time with the I-K bilinear model instead of the bilinear model. Comparison of the ratio of cumulative plastic deformation between the two models [Fig.12(a) (with isotropic-type hardening) versus Fig.7(a) (bilinear)] leads to the following observations: (1) the ratio of cumulative plastic deformation decreases somewhat when isotropic-type hardening is present, and this occurs because of the increase in apparent yield strength under repeated loading, as discussed in the previous section; and (2) distributions of the ratios along the stories are more uniform when isotropic-type hardening is present, and particularly when the ratio of second stiffness is small. Figures 12(b)-(d) show the distributions if the yield strength of one particular story (1st, 4th, or 7th story in the 9- story model) is weakened to 80% of the original, demonstrating that the ratio of cumulative plastic deformation increases for that weakened story, although the increase is less significant than for the corresponding bilinear systems [Fig.7(b)-(d)], particularly when the ratio of second stiffness is small. This behavior can be interpreted as follows. When one story is weaker and starts yielding earlier than other stories, the earthquake energy tends to be exerted concentrically into that story [as shown in Fig.7(b)-(d)]. When isotropic-type hardening is present, however, the yielding story is strengthened after experiencing

yielding and succeeding plastic deformation, which results in a higher chance of yielding and plastic deformation in other stories under successive cycles of loading. In summary, isotropic-type hardening associated with hysteretic dampers with the low-yield steel possesses the ability to self-adjust the story yield force to achieve uniform distribution of cumulative plastic deformations along the stories.

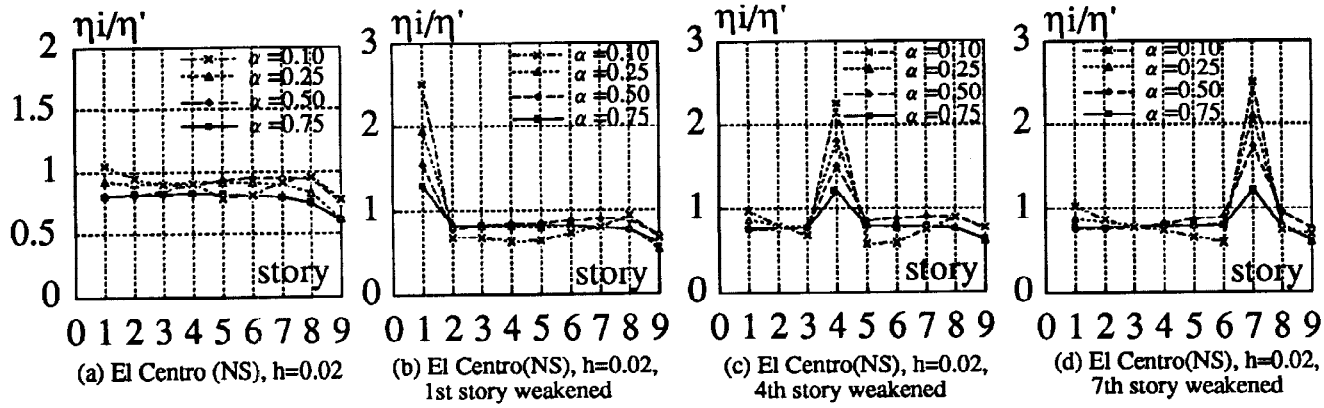


(a) El Centro (NS), h=0.02 (b) El Centro(NS), h=0.02, 1st story weakened (c) El Centro(NS), h=0.02, 4th story weakened (d) El Centro(NS), h=0.02, 7th story weakened

Fig.12. Distribution of cumulative plastic deformations obtained for I-K bilinear models.

## CONCLUSIONS

Energy input and dissipation characteristics of structures with hysteretic dampers made of the low-yield steel were examined, and the major findings are summarized as follows.

(1) Input and dissipated energies remain relatively unchanged regardless of the yield force and the ratio of second stiffness (up to $\alpha$ = 0.75 in this paper), which suggests that the basic premises of energy-based seismic design are applicable for structures with hysteretic dampers, which are characterized by large ratios of second stiffness.

(2) The larger is the ratio of second stiffness, the more uniformly the cumulative plastic deformation is distributed along the stories.

(3) Isotropic-type hardening inherent to hysteretic dampers made of the low-yield steel affects the total dissipated energy little, but tends to reduce the required cumulative plastic deformation because of the increase in apparent yield strength under repeated loading.

(4) Isotropic-type hardening is advantageous in making the distribution of cumulative plastic deformations along the stories more uniform than in the cases where such hardening is absent, and this trend is more conspicuous for smaller ratios of second stiffness. This behavior is achieved thanks to the strengthening associated with isotropic-type hardening under repeated loading.

## REFERENCES


Akiyama, H.(1985). *Earthquake-resistant limit-sate design of buildings*, University of Tokyo Press, Tokyo, Japan, 1985.

Housner, G. W.(1956). Limit design of structures to resist earthquakes, *Proceedings of the First World Conference on Earthquake Engineering*, Berkeley, CA, pp.5.1-5.13.

Nakashima, M., *et al.* (1994): Energy dissipation behavior of shear panels made of low-yield steel, *Journal of Earthquake Engineering and Structural Dynamics*, John-Wiley, **23**, pp.1299-1314.

Nakashima, M. (1995). Strain-hardening behavior of shear panels made of low-yield steel, I: test, *Journal of Structural Engineering*, ASCE, **121**, pp.1742-1749.

Nakashima, M., Akazawa, T. and Igarashi, H. (1995a). Pseudo-dynamic testing using conventional testing devices, *Journal of Earthquake Engineering and Structural Dynamics*, John-Wiley, **24**, pp.1409-1422.

Nakashima, M., Akazawa, T. and Tsuji, B. (1995b). Strain-hardening behavior of shear panels made of low-yield steel, II: model, *Journal of Structural Engineering*, ASCE, **121**, pp.1750-1757.

Nakashima, M., Saburi, K. and Tsuji, B (1996). Energy input and dissipation behavior of structures with hysteretic dampers, *Journal of Earthquake Engineering and Structural Dynamics*, John Wiley, **25** (in press).